



Effect of the mass ratio on the escape in the 4-body ring problem

Ibrahim Belgharbi, Juan F. Navarro^a

Department of Applied Mathematics, University of Alicante, Alicante, Spain

Received: 4 May 2022 / Accepted: 11 July 2022
© The Author(s) 2022

Abstract The aim of this paper is to analyze the effect of the mass ratio on the distribution of short times of escape and the probability of escape of a particle from the 4-body ring configuration. To this purpose, we carry out a numerical exploration of the problem, considering three different values of the mass ratio between the central and the primary bodies and, for each of these values, a pair of values of the Jacobi constant.

1 Introduction

The analysis of the geometric structures that govern the escape of a particle from an open Hamiltonian system has focused the efforts of many research groups over the last decades [1–8, 10, 11, 13–22, 24–26]. One of the systems that has aroused much of that interest is a particular case of the N -body problem: the N -body ring problem [18–22]. This attention is due to the fact that this system models a wide range of celestial systems, like planetary rings, asteroid belts and some type of formations of stars and planets, to cite some examples. This problem was first studied by Maxwell in 1859 [9], when addressing the understanding of the stability of Saturn's rings. Salo and Yoder [23] perform an analysis of the dynamical behavior of a coorbital satellite ring for $2 \leq N \leq 9$ satellites, finding that equally spaced rings are not stable under small perturbations for $N \leq 6$. They also show that there exists another stable compact stationary configuration, with angular separations not larger than $\pi/3$ between adjacent satellites, for $2 \leq N \leq 8$.

Also, Navarro and Martínez–Belda [20] carry out a numerical exploration of the N -body ring problem in order to analyze the distribution of times of escapes, for $N = 5, 6, 7, 8$ primaries, and considering a fixed value of the mass ratio $\beta = 2$. Moreover, they fulfill a detailed calculation of the basins of escapes for these four values of N . Navarro et al. [22] try to find out common properties in the escape from open Hamiltonian systems with the same number of openings in the potential well. In their work, they compare a galactic potential with the 4-body ring problem, pointing to a characteristic way in which the fast escape occurs in this type of systems. In this work, the authors show how the number of escaping orbits tends to zero as the time of escape becomes larger in both systems, despite of the fact that, for short times of escape, the distribution of the number of escaping orbits is significantly different in both systems. In the 4-body ring problem, this distribution appears to be approximately uniform and slowly decreasing with time, for times of escape from 0 to 40, and considering intervals of time of unit size. However, in the galactic system, the fast escape follows a sequential pattern. This different behavior is due to the shape of the geometric curves obtained when the stable manifolds to the Lyapunov orbits located at the openings of the curves of zero velocity are projected on the surfaces of section in both systems. In some sense, we can state that these projections have an ordered structure in the galactic system and a more intertwined architecture in the 4-body ring problem.

In the present paper, our interest focuses on the analysis of the way in which the value of the mass ratio and the Jacobi constant affect the distribution of fast times of escape, for a particular case of the number of bodies, $N = 4$. The numerical analysis that we present here has been carried out for the values of the mass ratio $\beta = 2, 10$ and 20 . For each of these values of the mass ratio, we have chosen two values of the Jacobi constant, so that the opening of the potential well has roughly the same size for the different values of β .

For the numerical exploration of the problem, we have defined grids of initial conditions in the region allowed by the value of the Jacobi constant on the surface of section $x = y, \dot{y} > 0$. For each of the initial conditions taken on these grids, we carry out a numerical integration of the problem up to a maximum time of integration of 100 units of time, since, as we have previously commented, our interest is restricted to the fast times of escape in order to clarify how the escape is related to with the sequence of the intersections of the stable and unstable manifolds associated to the Lyapunov orbits located at the openings of the potential well. If a particle has not left the system for an integration time of 100 units of time, we will consider that it remains trapped in it. In this way, we analyze the dependence of the distribution of short times of escape on β and C and, also, we show that the sequential pattern in the distribution of short times of escape that Navarro et al. [22] found in the galactic problem can also be found in the

^a e-mail: jf.navarro@ua.es (corresponding author)

4-body problem when the value of the Jacobi constant is close to its critical value and, then, the architecture of the projections of the stable manifolds to the Lyapunov orbits located at the openings of the potential well on the surface of section arises clearly.

2 Equations of motion and curves of zero velocity

The 4-body ring problem describes the motion of a point mass under the gravitational influence of 4 + 1 bodies. Four of these bodies (called peripheral primaries) have equal mass m and are located at the vertices of a regular polygon that rotates with constant angular velocity around the main body, with mass m_0 , which is located at the geometric center of this polygon. If we consider a barycentric synodic coordinate system Oxy rotating with the same angular velocity that the polygon which contains the primaries, the equations of motion that describe the motion in the plane defined by the 4 + 1 bodies are written as

$$\ddot{x} - 2\dot{y} = \frac{\partial U}{\partial x}, \quad \ddot{y} + 2\dot{x} = \frac{\partial U}{\partial y}, \quad (1)$$

where $U(x, y)$ is the potential

$$U(x, y) = \frac{1}{2}(x^2 + y^2) + \frac{1}{\Delta} \left(\frac{\beta}{r_0} + \sum_{\nu=1}^4 \frac{1}{r_\nu} \right), \quad (2)$$

$\beta = m_0/m$ is the mass ratio between the masses of the central and the peripheral primaries, $r_0 = \sqrt{x^2 + y^2}$, $r_\nu = \sqrt{(x - x_\nu^*)^2 + (y - y_\nu^*)^2}$, for $\nu = 1, 2, 3, 4$, and being x_ν^* and y_ν^* the coordinates of the peripheral primaries. These coordinates can be easily expressed as a function of the angle between the central body and two successive peripheral primaries [21, 22]. The Jacobi integral of motion C of this system is given by

$$C = 2U(x, y) - (\dot{x}^2 + \dot{y}^2). \quad (3)$$

The curves of zero velocity define the limits of the motion of the test particle under the influence of the gravitational configuration described above. These curves can be obtained through the relation

$$C = 2U(x, y). \quad (4)$$

As the square of the velocity of the particle must be nonnegative, the curves defined by Eq. (4) separate the (x, y) plane in regions where the motion of the particle is permitted and in regions where this motion is impossible to happen. Equations (2) and (4) show how the curves of zero velocity depend on the value of the ratio β and the Jacobi constant C . In our work, we have considered three values of β and, for each value of β , we have taken two values of C in order to analyze the dependence of the escape of the test particle on these two parameters. We have selected the value of the Jacobi constant of the system to obtain openings of approximately the same size in all the cases we have considered.

For each value of β , there exists a critical value of the Jacobi constant C_e such that the curves of zero velocity of the system open at four locations. If $C > C_e$, the curves of zero velocity are closed and particles cannot leave the potential but, when $C < C_e$, particles may leave the potential well through one of the four openings. Each of the openings of the curves of zero velocity is guarded by an unstable periodic orbit, called Lyapunov orbit. If a particle crosses outside of one of these four Lyapunov orbits, then it escapes from the system. The critical values for the values of β considered in this paper are

$$C_e(\beta = 2) = 2.751285, \quad C_e(\beta = 10) = 1.99511, \quad C_e(\beta = 20) = 1.81465.$$

In Fig. 1, we depict the curves of zero velocity for $N = 4$, $\beta = 2$, $C_1 = 2.748$ (Fig. 1a), $\beta = 2$, $C_2 = 2.751$ (Fig. 1d), $\beta = 10$, $C'_1 = 1.992$ (Fig. 1b), $\beta = 10$, $C'_2 = 1.995$ (Fig. 1e), $\beta = 20$, $C''_1 = 1.808$ (Fig. 1c), and $\beta = 20$, $C''_2 = 1.814$ (Fig. 1f). In Fig. 1a, we have labeled each of the four openings of the system to simplify the analysis of the problem.

3 Numerical exploration of the system

In order to carry out a numerical analysis of the escape of a particle from the 4-body configuration, we consider a set of initial conditions in the surface of section defined by $x = y$, $\dot{y} \geq 0$. In this surface of section, we define a grid of 512×512 equally spaced points in the region of the hyperplane (x, \dot{x}) allowed by the value of the Jacobi constant: if the values of the initial conditions x_0 and \dot{x}_0 are given, we set $y_0 = x_0$, and \dot{y}_0 is calculated by means of the relation

$$\dot{y}_0 = +\sqrt{2U(x_0, x_0) - C - \dot{x}_0^2}.$$

According to this, the initial conditions are taken in the domain D_β defined by

$$D_{\beta,C} = \{(x_0, \dot{x}_0) \in \mathbb{R}^2 : 2U(x_0, y_0) - C - \dot{x}_0^2 \geq 0\}. \quad (5)$$

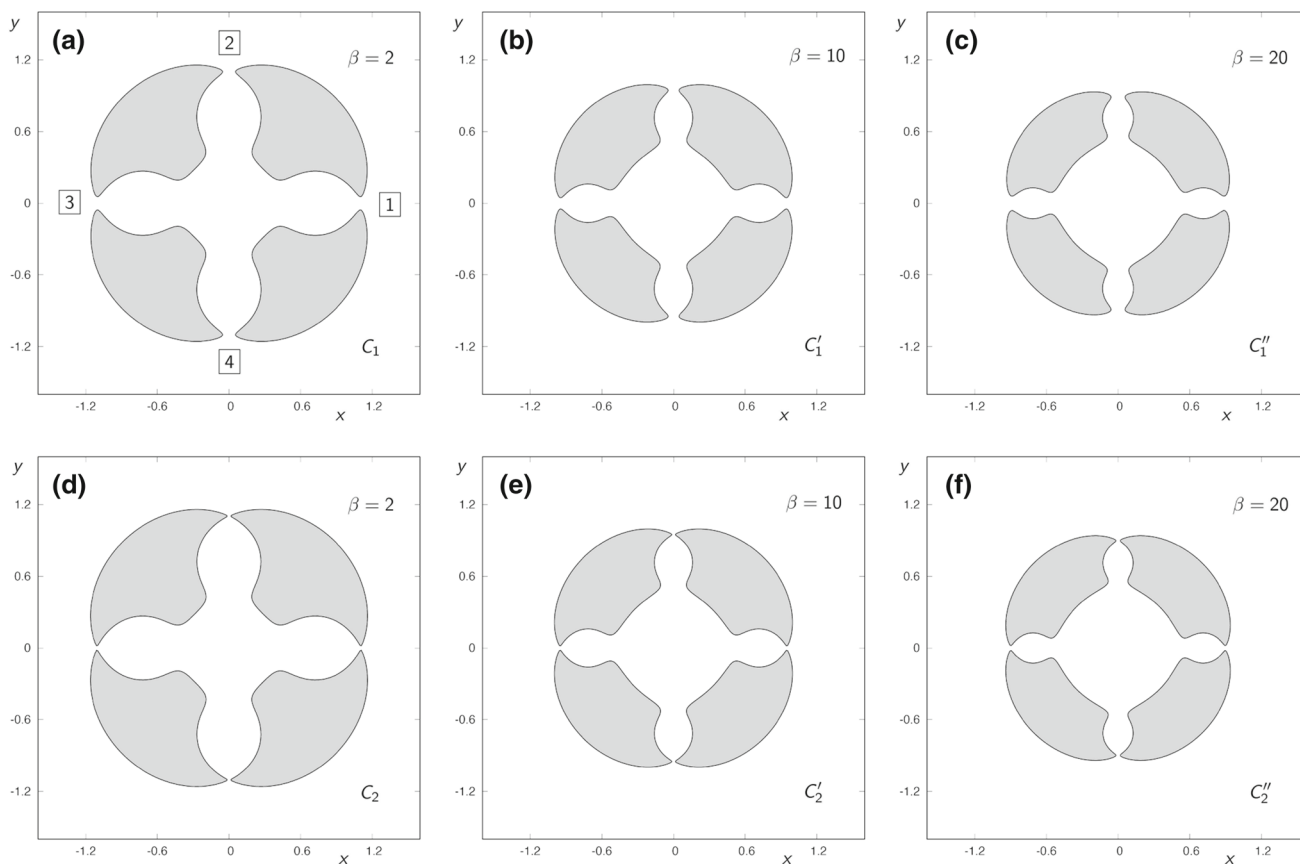


Fig. 1 Curves of zero velocity for $N = 4$ and: **a** $\beta = 2$, $C_1 = 2.748$, **b** $\beta = 10$, $C'_1 = 1.992$, **c** $\beta = 20$, $C''_1 = 1.808$, **d** $\beta = 2$, $C_2 = 2.751$, **e** $\beta = 10$, $C'_2 = 1.995$ and **f** $\beta = 20$, $C''_2 = 1.814$. We have colored in gray, the region where the motion of the particle cannot happen

As we have established above, we consider three values of the mass ratio β and a pair of values of the Jacobi constant and, thus, six domains, $D_{\beta=2,C=C_1}$, $D_{\beta=10,C=C'_1}$, $D_{\beta=20,C=C''_1}$, $D_{\beta=2,C=C_2}$, $D_{\beta=10,C=C'_2}$ and $D_{\beta=20,C=C''_2}$.

According to Navarro and Martínez-Belda [21], in order to study the distribution of the times of escape in these configurations of the 4-body ring problem, we consider a maximum time of integration of $T_{\max} = 10^2$. When integrating one initial condition in the domain of possible initial conditions in the surface of section, either the particle escapes from the system through one of the four openings with a time of escape smaller than T_{\max} , or it remains trapped in the potential well if the particle has not left the potential well in T_{\max} . The escape time t_{esc} is defined as the time a particle needs to cross one of the Lyapunov orbits with velocity pointing outwards. Orbits that do not escape after a numerical integration of T_{\max} units of time are considered as non-escaping or trapped orbits. We have employed the recurrent series power method to integrate the system numerically, as described in [12].

In the remaining part of this paper, $M(\beta, C)$ denotes the total number of initial conditions in the grid inside the domain $D_{\beta,C}$ when the value of the mass ratio and the Jacobi constant are given by β and C , respectively. Let β be the mass ratio and C the value of the Jacobi constant. Then, $E_\nu(\beta, C)$ denotes the number of orbits that leave the potential well through the opening ν , $E(\beta, C)$ denotes the total number of orbits that leave the potential well, $E_\nu(\beta, C, t_1, t_2)$ denotes the number of orbits that leave the potential well through the opening ν with a time of escape t such that $t_1 < t \leq t_2$, $E(\beta, C, t_1, t_2)$ denotes the number of orbits that leave the potential well with a time of escape t such that $t_1 < t \leq t_2$. Moreover, $E_\nu(\beta, C, t)$ denotes the total number of orbits that escape through the opening ν with a time of escape smaller than t , and $E(\beta, C, t)$ the total number of orbits that escape from the system with a time of escape smaller than t . The following relations are satisfied:

$$E_\nu(\beta, C, t) = E_\nu(\beta, C, 0, t), \quad E(\beta, C, t) = E(\beta, C, 0, t) = \sum_{\nu=1}^4 E_\nu(\beta, C, t),$$

$$E_\nu(\beta, C) = E_\nu(\beta, C, T_{\max}), \quad E(\beta, C) = E(\beta, C, T_{\max}),$$

for any $\nu = 1, 2, 3, 4$. Finally, $P_\nu(\beta, C, t_1, t_2)$ denotes the probability of escape through the opening ν with a time of escape t such that $t_1 < t \leq t_2$, $P(\beta, C, t_1, t_2)$ denotes the probability of escape of a particle from the system with a time of escape t such that $t_1 < t \leq t_2$, $P_\nu(\beta, C, t)$ denotes the probability of escape through the opening ν with a time of escape smaller than t , and $P(\beta, C, t)$ denotes the probability of escape with a time of escape smaller than t . Thus,

Table 1 Number of initial conditions numerically integrated for each value of β and C , together with the number of escaping orbits and the probability of escape, considering $T_{\max} = 100$

	$\beta = 2$		$\beta = 10$		$\beta = 20$	
	$C_1 = 2.748$	$C_2 = 2.751$	$C'_1 = 1.992$	$C'_2 = 1.995$	$C''_1 = 1.808$	$C''_2 = 1.814$
$M(\beta, C)$	222 554	221 914	234 648	234 056	234 564	233 304
$E(\beta, C, T_{\max})$	34 831	4 595	27 433	4 296	30 169	2 632
$P(\beta, C, T_{\max})$	0.1565	0.0207	0.1169	0.0184	0.1286	0.0241

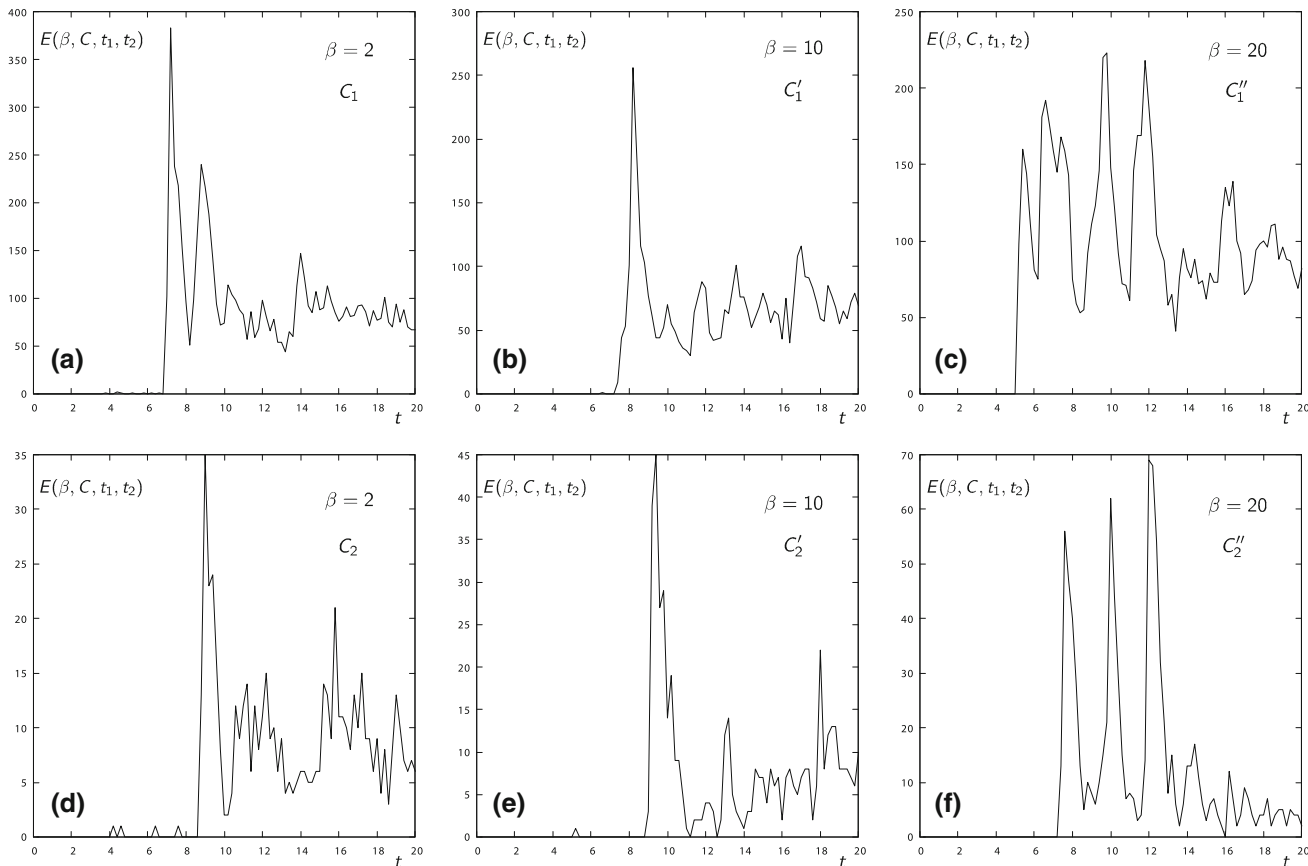


Fig. 2 **a** $E(\beta = 2, C_1, t_1, t_2)$, **b** $E(\beta = 10, C'_1, t_1, t_2)$, **c** $E(\beta = 20, C''_1, t_1, t_2)$, **d** $E(\beta = 2, C_2, t_1, t_2)$, **e** $E(\beta = 10, C'_2, t_1, t_2)$, **f** $E(\beta = 20, C''_2, t_1, t_2)$, considering $t_1 = nh, t_2 = (n + 1)h$, being $h = 0.2$ and $n \in \mathbb{N}, 0 \leq n \leq 99$

$$P_v(\beta, C, t_1, t_2) = \frac{E_v(\beta, C, t_1, t_2)}{M(\beta, C)}, \quad P(\beta, C, t_1, t_2) = \frac{E(\beta, C, t_1, t_2)}{M(\beta, C)}, \quad P_v(\beta, C, t) = \frac{E_v(\beta, C, t)}{M(\beta, C)},$$

and

$$P(\beta, C, t) = \frac{E(\beta, C, t)}{M(\beta, C)}.$$

Table 1 summarizes the number of initial conditions we have integrated in each case, together with the number of escaping orbits and the probability of escape, considering $T_{\max} = 100$. In this table, we can see that when the value of the mass ratio goes from $\beta = 2$ to $\beta = 10$, the probability of escape decreases. However, when we go from $\beta = 10$ to $\beta = 20$, the probability of escape increases slightly. This tendency occurs for the two values of the Jacobi constant that we have considered. This means that the probability of escape does not vary monotonically with the mass ratio β .

Now, we focus our analysis on the orbits that escape from the system with times of escape smaller than 20 units of time. We consider short times of escape because we are interested in the distribution of the times of fast escape from the system. Thus, we have computed the following quantities: $E_v(\beta = 2, C_1 = 2.748, t_1, t_2)$, $E(\beta = 2, C_1 = 2.748, t_1, t_2)$, $E_v(\beta = 2, C_2 = 2.751, t_1, t_2)$, $E(\beta = 2, C_2 = 2.751, t_1, t_2)$, $E_v(\beta = 10, C'_1 = 1.992, t_1, t_2)$, $E(\beta = 10, C'_1 = 1.992, t_1, t_2)$, $E_v(\beta = 10, C'_2 = 1.995, t_1, t_2)$, $E(\beta = 10, C'_2 = 1.995, t_1, t_2)$, $E_v(\beta = 20, C''_1 = 1.808, t_1, t_2)$, $E(\beta = 20, C''_1 = 1.808, t_1, t_2)$, $E_v(\beta = 20, C''_2 = 1.814, t_1, t_2)$, $E(\beta = 20, C''_2 = 1.814, t_1, t_2)$.

and $E(\beta = 20, C_2'' = 1.814, t_1, t_2)$, for $v = 1, 2, 3, 4$, and considering $t_1 = nh, t_2 = (n + 1)h$, being $h = 0.2$ and $n \in \mathbb{N}, 0 \leq n \leq 99$. In Fig. 2a–d, we depict $E(\beta = 2, C_1 = 2.748, t_1, t_2)$ and $E(\beta = 2, C_2 = 2.751, t_1, t_2)$, respectively. In Fig. 2b–e, we show $E(\beta = 10, C_1' = 1.992, t_1, t_2)$ and $E(\beta = 10, C_2' = 1.995, t_1, t_2)$. Finally, Fig. 2c–f show $E(\beta = 20, C_1'' = 1.808, t_1, t_2)$ and $E(\beta = 20, C_2'' = 1.814, t_1, t_2)$. In all these figures, we have taken $t_1 = nh$ and $t_2 = (n + 1)h, h = 0.2$ and $n \in \mathbb{N}, 0 \leq n \leq 99$.

Our computations unveil that, when $\beta = 2$ and $C_1 = 2.748$, 6741 initial conditions correspond to orbits that escape from the potential well with times of escape smaller than $T_{\max} = 20$. This means that 3.03% of the orbits escape. Figure 2a shows that, when $\beta = 2$ and $C_1 = 2.748$, there are no escaping orbits with times of escape in the interval $(0, 3.6]$, and only 8 orbits with times of escape in the interval $(3.6, 6.8]$. In the interval $(6.8, 7]$, we find 102 escaping orbits and, right after that, we find a main peak of 383 orbits with times of escape in the interval $(7, 7.2]$. Then, in the interval $(7.2, 8.2]$, the number of escaping orbits descends to 51 orbits and we find a secondary peak of 240 orbits that leave the system in the interval $(8.2, 8.8]$. After that, the number of escaping orbits per interval of time oscillates following a step by step pattern. The average number of escaping orbits seems to be constant until $T_{\max} = 20$. For $\beta = 2$ and $C_2 = 2.751$, 556 of the orbits escape from the potential well, that is, 0.25% of the orbits. Figure 2d shows that, when $\beta = 2$ and $C_2 = 2.751$, there are no orbits with times of escape in the interval $(0, 4]$, and only 4 orbits in the interval $(4, 8.6]$. The number of escaping orbits increases to 35 orbits at $t = 9$ and, then, it descends until 2 escaping orbits at $t = 10$. In the intervals $(10, 13]$ and $(15, 20]$, the escape occurs in a sequential manner. In the interval $(13, 15]$, the number of escaping orbits in each of the 10 intervals we have considered is bounded between 4 and 6 orbits.

When $\beta = 10$ and $C_1' = 1.992$, 4528 of the orbits escape, that is, 1.93% of the orbits. For $\beta = 10$ and $C_2' = 1.995$, only 484 orbits escape, corresponding to 0.2067% of the orbits we have integrated. Figure 2b shows that, when $\beta = 10$ and $C_1' = 1.992$, there is only one orbit that leaves the potential well with a time of escape in the interval $(0, 7.2]$. To be more precise, this orbit has a time of escape between $t_1 = 6.4$ and $t_2 = 6.6$. In the interval $(7.4, 8.2]$, the number of escaping orbits increases to reach the peak of 256 orbits in the last period of this interval, and it decreases to 44 orbits in the interval $(8.2, 9.6]$. In the interval $(9.6, 20]$, the escape occurs following a sequential pattern, with a number of escaping orbits per interval of time oscillating between 34 and 116 orbits. Figure 2e shows that, when $\beta = 10$ and $C_2' = 1.995$, there is just one escaping orbit in the interval $(0, 8.8]$, with a time of escape between $t = 5$ and $t = 5.2$. In the interval $(8.8, 9.4]$, the number of escaping orbits increases to 45 orbits, which is the peak for this case. Then, in the interval $(9.4, 11.2]$, the number of escaping orbits descends to 0 in an irregular way, increasing and decreasing alternatively many times. After that, the number of escaping orbits per interval of time oscillates following a step by step pattern and presenting several secondary peaks.

When $\beta = 20$ and $C_1'' = 1.808$, 8165 of the orbits leave the potential well, what means that 3.48% of the orbits escape. Figure 2c shows that, when $\beta = 20$ and $C_1'' = 1.808$, we find several primary peaks of escaping orbits per interval of time. We do not find any escaping orbit in the interval $(0, 5]$ and, in the interval $(5, 13.4]$, we can observe that there are four main peaks. In this case, it is obvious that the escape occurs in an irregular step by step way. Finally, when $\beta = 20$ and $C_2'' = 1.814$, 923 of the orbits leave the potential well, corresponding to 0.3956% of the orbits. Figure 2f shows that, when $\beta = 20$ and $C_2'' = 1.814$, we have two periods where the escape follows a step by step pattern. In the interval $(0, 7.2]$, there are no escaping orbits. Then, we find three main peaks in ascending order, the third of them in the interval $(7.4, 8.6]$, when the number of escaping orbits increases to 56 orbits and, then, it decreases to 5 escaped orbits.

We can conclude that the value of β affects the evolution of the number of escaping orbits. We observe that for the three values of the parameter β that we have considered, and considering values of the Jacobi constant corresponding to openings of the same size, the distribution of the number of escaping orbits per interval of time presents some differences. We have found that for $\beta = 2$ and $\beta = 10$, there is a main peak very pronounced and centered at a time of escape between 7 and 9 units of time and, for longer times of escape, the number of orbits that escape oscillates following a sequential pattern. However, for $\beta = 20$, we have found three main peaks, with an average separation between them of 3 units of time. From there, the behavior of the number of escaping orbits per interval of time is quite similar to that of the other two values of the mass ratio. On the other hand, when we consider, for the same value of β , two different values of the Jacobi constant, we see how, in essence, the shape of the curve is the same, although as the size of the opening decreases, the architecture underlying the distribution of the number of escaping orbits with respect to time it is shown more clearly.

In order to clarify the mechanism that explains the way particles escape from the system, we will look into a pair of the cases with more detail. In particular, we analyze the escape for $\beta = 2, C = C_2$ and $\beta = 20, C = C_2''$.

Figure 3 shows the number of escaping orbits per interval of time for $\beta = 2$ and $C = C_2$ through the first (Fig. 3a), second (Fig. 3b), third (Fig. 3c) and fourth (Fig. 3d) openings. We find the main peak in the number of escaping orbits per interval of time in the second opening of the curves of zero velocity. In Fig. 3c, we can observe clearly how the distribution of the times of escape is grouped around several centers. Indeed, there are four intervals where the number of escaping orbits stays constant in the interval $(12.8, 16.2]$. Regardless of the number of orbits that escape through each of the openings, we can conclude that the escape occurs sequentially.

Figure 4 shows the number of escaping orbits per interval of time for $\beta = 20$ and $C = C_2''$ through the first (Fig. 4a), second (Fig. 4b), third (Fig. 4c) and fourth (Fig. 4d) openings. First, we note that, in the first three openings, the number of escaping orbits per interval of time has a main peak: the sum of these three peaks explains the three main peaks depicted in Fig. 2f. Finally, we can observe that the escape through the fourth opening occurs following a very accentuated sequential pattern. Although the same occurs in the four openings, in the fourth opening is shown much more clearly.

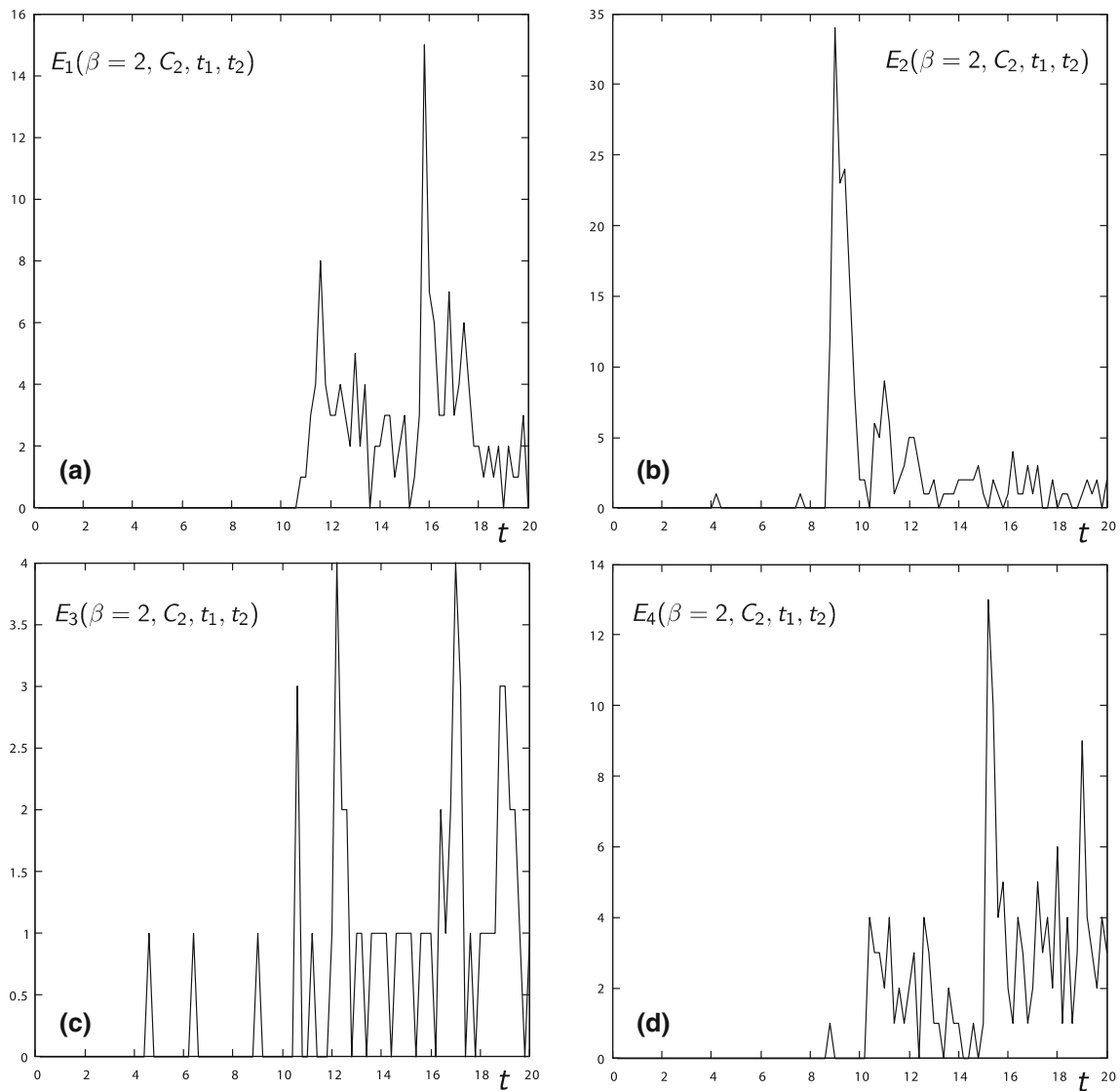


Fig. 3 **a** $E_1(\beta = 2, C_2, t_1, t_2)$, **b** $E_2(\beta = 2, C_2, t_1, t_2)$, **c** $E_3(\beta = 2, C_2, t_1, t_2)$, **d** $E_4(\beta = 2, C_2, t_1, t_2)$, for $C_2 = 2.751$, and considering $t_1 = nh$, $t_2 = (n + 1)h$, being $h = 0.2$ and $n \in \mathbb{N}$, $0 \leq n \leq 99$

In both cases (Figs. 3 and 4), the sequence pattern we have found in the distribution of the number of escaping orbits per interval of time has its origin in the way the stable manifolds to the Lyapunov orbits located at the openings of the curves of zero velocity intersect the surface of section. We have observed that three of the openings have a similar behavior: there are three values of $t = \bar{t}_\nu$, with $\nu = \nu_1, \nu_2, \nu_3$, being $\nu_1, \nu_2, \nu_3 \in \{1, 2, 3, 4\}$, at which the number of escaping orbits reaches a maximum. These values of time \bar{t}_ν , with $\nu = \nu_1, \nu_2, \nu_3$, correspond to the average time the stable manifold to the Lyapunov orbits located at the ν -th openings of the potential needs to intersect the surface of section when we integrate them backward. Each of the openings has a different time \bar{t}_ν , as the crossing time of each of the stable manifolds with the surface of section is different. From this value of $t = \bar{t}$, the number of escaping orbits descends drastically to become stable, showing an oscillating and sequential behavior. In both of the cases depicted in Figs. 3 and 4, one of the openings (the third opening for $\beta = 2$ and the fourth opening for $\beta = 20$) presents a different behavior: the escape occurs sequentially, step by step, as described above.

For a better understanding of this result, we show in Fig. 5a a joint representation of the number of escaping orbits for the three values of the mass ratio and the two values of the Jacobi constant we have considered, for a maximum time of integration $T_{\max} = 100$. Moreover, In Fig. 5b, we give the probabilities of escape. In both graphics, we have considered $t_1 = nh$, $t_2 = (n + 1)h$, being $h = 1$ and $n \in \mathbb{N}$, $0 \leq n \leq 99$. We have depicted each case in a different color: purple for $\beta = 2$ and $C_1 = 2.748$, black for $\beta = 2$ and $C_2 = 2.751$, dark blue for $\beta = 10$ and $C'_1 = 1.992$, dark red for $\beta = 10$ and $C'_2 = 1.995$, yellow for $\beta = 20$ and $C''_1 = 1.808$ and dark green for $\beta = 20$ and $C''_2 = 1.814$. The value $T_{\max} = 100$ has been chosen to ease the comparison between

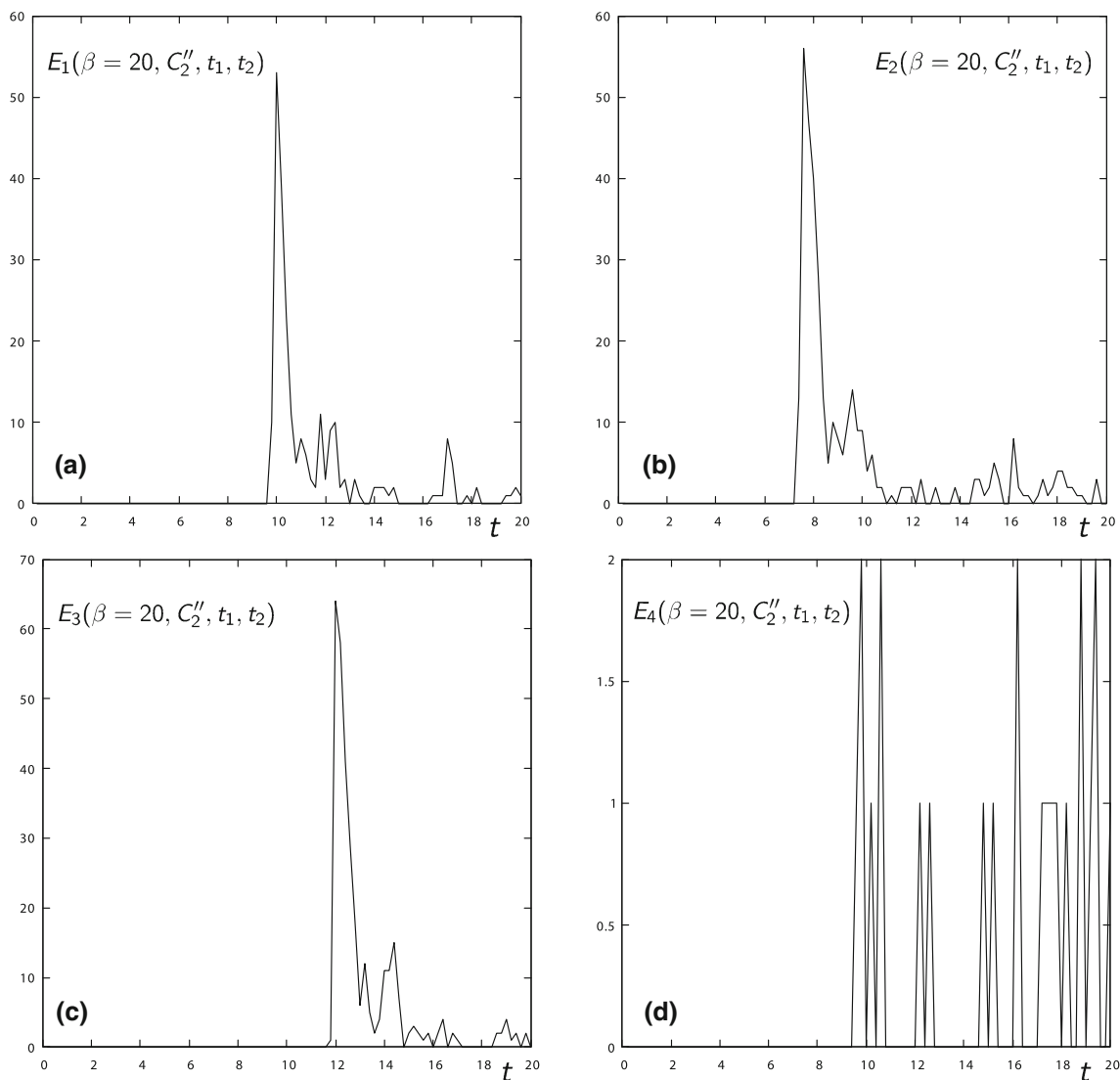


Fig. 4 **a** $E_1(\beta = 20, C_2'', t_1, t_2)$, **b** $E_2(\beta = 20, C_2'', t_1, t_2)$, **c** $E_3(\beta = 20, C_2'', t_1, t_2)$, **d** $E_4(\beta = 20, C_2'', t_1, t_2)$, for $C_2'' = 2.751$, and considering $t_1 = nh$, $t_2 = (n + 1)h$, being $h = 0.2$ and $n \in \mathbb{N}$, $0 \leq n \leq 99$

the evolution of the number of escaping orbits and the probability of escape for the different values of the mass ratio. Moreover, the trend in the evolution of these two quantities with time is unveiled by using this value of T_{max} .

In Fig. 5a, we can observe that there is an average almost constant difference between the number of escaping orbits per interval of time for $\beta = 2, C = C_1$ and $\beta = 10, C = C'_1$, corresponding with the values of the Jacobi constant related to the biggest openings of the potential well. When we observe the evolution of the number of escaping orbits for $\beta = 20$ and $C = C''_1$, we distinguish that the yellow line has a steeper slope and, for $t = T_{max}$, we find almost the same difference between the three values of the number of escaping orbits associated to the Jacobi constants C_1, C'_1 and C''_1 . As the size of the opening becomes smaller, that is, for the Jacobi constants given by C_2, C'_2 and C''_2 , the number of escaping orbits tends to be approximately the same on average, unless they present an oscillating behavior.

In Fig. 5b, we observe different trends in the evolution of the probability of escape with respect to time. This is the reason why we have included in Fig. 6 two graphics, separating the probabilities of escape into two groups. On the one hand, we depict the probabilities of escape for C_1, C'_1 and C''_1 in Fig. 6a. On the other hand, Fig. 6b shows the probabilities of escape for C_2, C'_2 and C''_2 .

In Fig. 6a, we observe that the evolution of the probability of escape with respect to time is almost the same on average for $\beta = 2$ and $\beta = 10$. However, for $\beta = 20$, we find a steeper slope in the decrease of the probability of escape with respect to time. We also see that, for $\beta = 20$, the probability of escape is larger than those for $\beta = 2$ and $\beta = 10$, if we consider small times of escape. In Fig. 6b, we observe an initial difference in the probabilities that disappears as time grows.

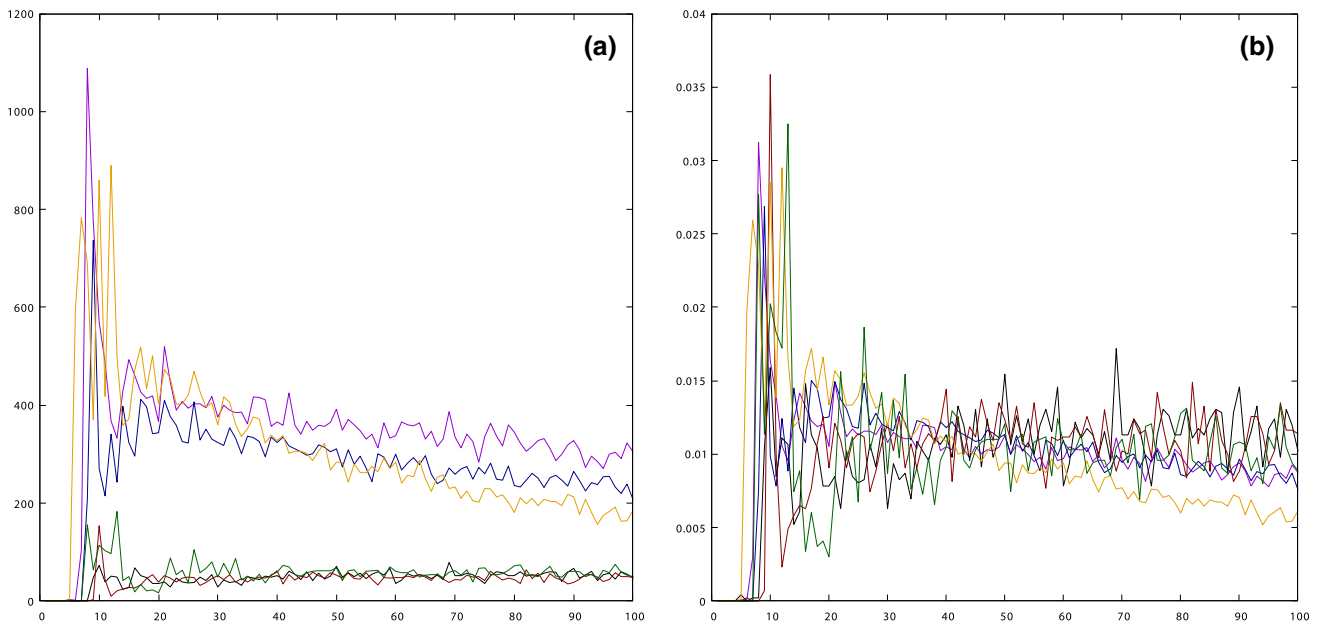


Fig. 5 **a** $E(\beta, C, t_1, t_2)$, **b** $P(\beta, C, t_1, t_2)$. We have used the following color code: purple for $\beta = 2$ and $C_1 = 2.748$, black for $\beta = 2$ and $C_2 = 2.751$, dark blue for $\beta = 10$ and $C'_1 = 1.992$, dark red for $\beta = 10$ and $C'_2 = 1.995$, yellow for $\beta = 20$ and $C''_1 = 1.808$ and dark green for $\beta = 20$ and $C''_2 = 1.814$. Here, we have considered $t_1 = nh, t_2 = (n + 1)h$, being $h = 1$ and $n \in \mathbb{N}, 0 \leq n \leq 99$

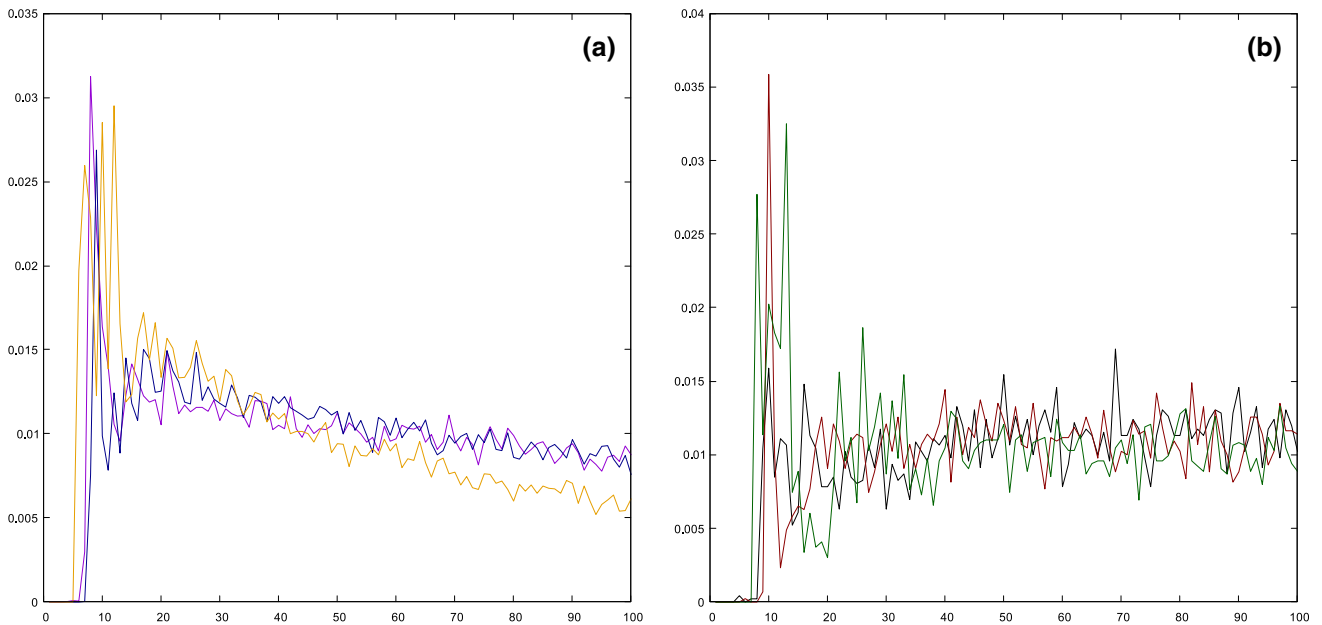


Fig. 6 **a** $P(\beta, C, t_1, t_2)$ for C_1, C'_1 and C''_1 and **b** $P(\beta, C, t_1, t_2)$ for C_2, C'_2 and C''_2 . We have used the following color code: purple for $\beta = 2$ and $C_1 = 2.748$, black for $\beta = 2$ and $C_2 = 2.751$, dark blue for $\beta = 10$ and $C'_1 = 1.992$, dark red for $\beta = 10$ and $C'_2 = 1.995$, yellow for $\beta = 20$ and $C''_1 = 1.808$ and dark green for $\beta = 20$ and $C''_2 = 1.814$. Here, we have considered $t_1 = nh, t_2 = (n + 1)h$, being $h = 1$ and $n \in \mathbb{N}, 0 \leq n \leq 99$

These results confirm that the probability of escape from this system does not depend on the mass ratio monotonically and, also, suggest the need to carry out a more detailed numerical exploration, considering more values of the mass ratio β in order to establish the mechanism that produces the change of behavior we have found for $\beta = 20$.

4 Conclusions

In this paper, we have started a numerical exploration of the escape in the 4-body ring problem, considering three values of the mass ratio β and two values of the Jacobi constant for each of the values of the mass ratio. To this purpose, we have integrated a mesh of 512×512 equally spaced initial conditions in the surface of section defined by $x = y, \dot{y} \geq 0$, determining, for each initial condition, if the corresponding orbit escapes from the system or remains trapped forever.

The results we have obtained unveil that the number of escaping orbits becomes similar in all the cases, for the values of the Jacobi constant related to the smallest openings of the curves of zero velocity. We have also found that the fast escape from the system occurs following a sequential pattern in all these three cases. When we consider the values of the Jacobi constant corresponding to the biggest openings of the potential, we have found some differences in the distribution of the number of escaping orbits for the three values of the mass ratio, and the same happens with the probabilities of escape. As in the case of the smallest openings, we have also found a sequential pattern in the distribution of the times of escape from the system.

These results suggest the need to carry out a more detailed numerical exploration, considering a sequence of values of the mass ratio that allows us to monitor the dependence of the behavior of the probability of escape on this parameter.

Funding Open Access funding provided thanks to the CRUE-CSIC agreement with Springer Nature.

Declarations

Conflict of interest This work does not have any conflicts of interest.

Open Access This article is licensed under a Creative Commons Attribution 4.0 International License, which permits use, sharing, adaptation, distribution and reproduction in any medium or format, as long as you give appropriate credit to the original author(s) and the source, provide a link to the Creative Commons licence, and indicate if changes were made. The images or other third party material in this article are included in the article's Creative Commons licence, unless indicated otherwise in a credit line to the material. If material is not included in the article's Creative Commons licence and your intended use is not permitted by statutory regulation or exceeds the permitted use, you will need to obtain permission directly from the copyright holder. To view a copy of this licence, visit <http://creativecommons.org/licenses/by/4.0/>.

References

1. J. Aguirre, J.C. Vallejo, M.A.F. Sanjuan, Wada basins and chaotic invariant sets in the Hénon-Heiles system. *Phys. Rev. E* **64**, 066208 (2001)
2. J. Aguirre, M.A.F. Sanjuan, Limit of small exits in open Hamiltonian systems. *Phys. Rev. E* **67**, 056201 (2003)
3. B. Barbanis, Escape regions of a quartic potential. *Celest. Mech. Dyn. Astron.* **48**(1), 57–77 (1990)
4. R. Barrio, F. Blesa, S. Serrano, Fractal structures in the Hénon-Heiles Hamiltonian. *Europhys. Lett.* **82**, 10003 (2008)
5. R. Barrio, F. Blesa, S. Serrano, Bifurcations and safe regions in open Hamiltonians. *New J. Phys.* **11**, 053004 (2009)
6. G. Contopoulos, Asymptotic curves and escapes in Hamiltonian systems. *Astron. Astrophys.* **231**(1), 41–45 (1990)
7. G. Contopoulos, D. Kaufmann, Types of escapes in a simple Hamiltonian system. *Astron. Astrophys.* **253**(2), 379–388 (1992)
8. A.P.S. De Moura, P.S. Letelier, Fractal basins in Hénon-Heiles and other polynomial potentials. *Phys. Lett. A* **256**, 362–368 (1999)
9. J.C. Maxwell, *On the stability of motions of Saturn's rings* (Macmillan and Company, Cambridge, 1859)
10. J.F. Navarro, J. Henrard, Spiral windows for escaping stars. *Astron. Astrophys.* **369**, 1112–1121 (2001)
11. J.F. Navarro, Windows for escaping particles in quartic galactic potentials. *Appl. Math. Comput.* **303**, 190–202 (2017)
12. J.F. Navarro, Numerical integration of the N -body ring problem by recurrent power series. *Celest. Mech. Dyn. Astr.* **130**, 16 (2018)
13. J.F. Navarro, On the escape from potentials with two exit channels. *Sci. Rep.* **9**, 13174 (2019)
14. J.F. Navarro, On the integration of an axially symmetric galaxy model. *Comp. and Math. Methods* **1**(6), e1062 (2019)
15. J.F. Navarro, Limiting curves in an axially symmetric galaxy. *Math. Meth. Appl. Sci.* **44**, 993–1002 (2021)
16. J.F. Navarro, Dependence of the escape from an axially symmetric galaxy on the energy. *Sci. Rep.* **11**, 8427 (2021)
17. J.F. Navarro, A proper surface of section to study a new Hénon-Heiles potential with additional singular gravitational terms. *Eur. Phys. J. Plus* **136**, 537 (2021)
18. J.F. Navarro, M.C. Martínez-Belda, On the use of surfaces of section in the N -body problem. *Math. Meth. Appl. Sci.* **43**, 2289–2300 (2020)
19. J.F. Navarro, M.C. Martínez-Belda, Escaping orbits in the N -body ring problem. *Comp. and Math. Methods* **2**, e1067 (2020)
20. J.F. Navarro, M.C. Martínez-Belda, On the analysis of the fractal basins of escape in the N -body ring problem. *Comp. and Math. Methods* **3**, e1131 (2020)
21. J.F. Navarro, M.C. Martínez-Belda, Analysis of the distribution of times of escape in the N -body ring problem. *J. Comput. Appl. Math.* **404**, 113396 (2022)
22. J.F. Navarro, I. Belgharbi, M.C. Martínez-Belda, Analysis of the escape in systems with four exit channels. *Math. Meth. Appl. Sci.* 1–13 (2022)
23. H. Salo, C.F. Yoder, The dynamics of Coorbital satellite systems. *Astron. Astrophys.* **205**, 309–327 (1988)
24. C. Siopsis, H.E. Kandrup, G. Contopoulos, R. Dvorak, Universal properties of escape in dynamical systems. *Celest. Mech. Dyn. Astron.* **65**(1–2), 57–68 (1996)
25. E.E. Zotos, Trapped and escaping orbits in an axially symmetric galactic-type potential. *PASA* **29**, 161–173 (2012)
26. E.E. Zotos, W. Cheng, J.F. Navarro, T. Saeed, A new formulation of the Hénon-Heiles potential with additional singular gravitational terms. *Int. J. Bifurcation Chaos* **30**(13), 2050197 (2020)